Attitude Maneuver Control of Flexible Spacecraft by Observer-based Tracking Control

Hyochoong Bang*, Choong-Seok Oh
Division of Aerospace Engineering, KAIST
373-1, Kusong-Dong, Yousong-Gu, Daejon 305-701, Korea

A constraint equation-based control law design for large angle attitude maneuvers of flexible spacecraft is addressed in this paper. The tip displacement of the flexible spacecraft model is prescribed in the form of a constraint equation. The controller design is attempted in the way that the constraint equation is satisfied throughout the maneuver. The constraint equation leads to a two-point boundary value problem which needs backward and forward solution techniques to satisfy terminal constraints. An observer-based tracking control law takes the constraint equation as the input to the dynamic observer. The observer state is used in conjunction with the state feedback control law to have the actual system follow the observer dynamics. The observer-based tracking control law eventually turns into a stabilized system with inherent nature of robustness and disturbance rejection in LQR type control laws.

Key Words: Flexible Spacecraft Attitude Control, Constrain Equation, Tip Displacement, Two-point Boundary Value Problem, Observer-based Tracking Control Law, LQR

1. Introduction

Attitude control of flexible spacecraft has received significant attention during last decades (Breakwell, 1981). The flexible spacecraft are represented by on-board structures such as antenna and solar arrays. The typical spacecraft model consists of a center rigid body and flexible structures attached to the center body (Breakwell, 1981; VanderVelde et al., 1983). Majority of research effort has been concentrated on such a model.

Attitude maneuver of the flexible spacecraft causes dynamic interaction between the flexible parts and rigid center body, which prevents precision pointing of the on-board payloads (Meirovitch, 1987; Singh et al., 1989). For instance, Earth observation optical cameras should be free of vibration for high resolution image mapping missions. For stereo image acquisition missions, frequent and rapid large angle attitude maneuvers of spacecraft are to be executed. Light flexible structures tend to cause residual vibration, and it will increase total maneuver time until complete settling of the vibration. Thus the rapid attitude maneuver performance is strongly tied to the on-board flexible structures dynamics (Singh et al., 1989).

There has been a lot of research and investigation effort for such a problem. Numerical techniques have be been reported with analysis and experimental verification. Particular attention has been paid to the simultaneous large angle attitude maneuver with vibration suppression (Vadali, 1984; Byers et al., 1989). The control laws design has been heavily populated by finite dimensional mathematical model-based approaches (Wie et al., 1993). Some high authority control techniques such as LQR and other frequency domain designs

* Corresponding Author,
E-mail: hcbang@fdcl.kaist.ac.kr
TEL: +82-42-869-3722; **FAX**: +82-42-869-3710
Division of Aerospace Engineering, KAIST 373-1, Kusong-Dong, Yousong-Gu, Daejon 305-701, Korea
(Manuscript **Received** March 31, 2003; **Revised** September 3, 2003)

have been attempted (Breakwell, 1981). One key disadvantage of the model-based control laws is robustness with respect to modeling errors and uncertainties. Many robustified design methods for the model-based control laws are available (Wie, et al., 1993; Agrawal and Bang, 1995). Robust control law also has been investigated recently by Sung (2001).

On the other hand, output feedback based upon the Lyapunov stability theory has been also extensively investigated (Fujii et al., 1989; Junkins et al., 1991). Both analytical development and ground experimental verifications were reported (Junkins et al., 1991; Kim et al., 1997). The principal advantages of the output feedback control laws are primarily characterized by robustness and easy implementation. An output feedback form tracking control law using a smoothed reference trajectory showed highly satisfactory performance. Inverse dynamic method has been also investigated by using a flexible link system model. The tip displacement is specified a priori, and a control law is designed in such a way that the tip constraint is satisfied. The control law design was conducted largely over frequency domain, and excessive computational burden was required.

In this paper, we propose a control law design method for the attitude maneuver of a flexible spacecraft model. The tip displacement about the inertial frame of reference is defined, and a stabilizing control law is designed to satisfy the given constraint rigorously. The reference trajectory generation is based upon a pure smoothed rigid body motion without vibration. The formulation of optimal control theory turns out to be a two-point boundary value problem with initial and terminal boundary conditions defined at separate time instants (Bryson, 1999). Derivation of the two-point value problem and associated numerical solution techniques are proposed. Direct solution for the two-point boundary value problem, however, is not easy and requires heavy storage for actual implementation. Consequently, they are not actually implemented due to the difficulty in numerical computation.

An observer-based tracking control law is a stabilized feedback system with the constraint equation satisfied rigorously. Thus main analysis in this paper is focused on the observer-based tracking control approach. Two-stage design — a dynamic observer and state feedback, ensures a stable closed-loop system by taking advantage of conventional LQR type design technique. Simulation results for observer-based tracking control are presented to validate the proposed method.

2. Dynamics and Modeling

2.1 Attitude dynamics

First, attitude dynamics for a flexible spacecraft model are presented. The spacecraft model configuration is shown in Fig. 1.

Two solar arrays are attached to the center body. The center body is subject to a single-axis rotational motion (θ). The control torque (u) is applied to the center body. The solar arrays tend to vibrate due to the coupling effect with the rigid body rotation. They are simplified as flexible beams with tip masses. The solar array flexibility is reflected into the beam, and the frequencies of oscillation are tuned by the tip masses. It is assumed that two solar arrays are identical in geometric and material properties. Under the torque control input only to the center body, the deflection of each solar array should be identical.

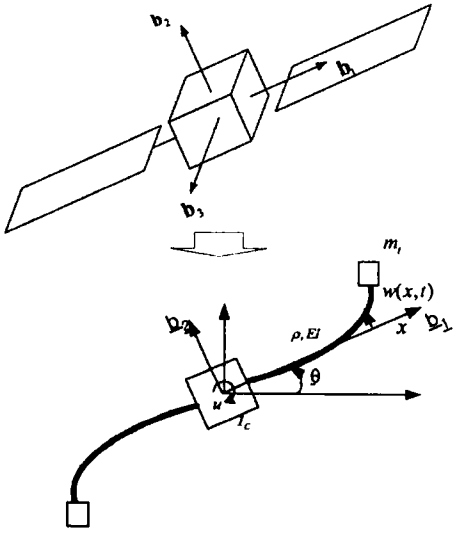

Fig. 1 Spacecraft model with single-axis rotation

Namely, the deflection takes place in an anti-symmetric fashion.

The original governing equations of motion for the spacecraft model are given by (Junkins et al., 1991)

$$I_c\ddot{\theta}+2\int_h^l \rho x\left(x\ddot{\theta}+\frac{\partial^2 w}{\partial t^2}\right)dx+2m_t l\left(l\ddot{\theta}+\frac{\partial^2 w}{\partial t^2}\Big|_l\right)=u$$
$$\rho\left(x\ddot{\theta}+\frac{\partial^2 w}{\partial t^2}\right)+EI\frac{\partial^4 w}{\partial x^4}=0 \quad (1)$$

where I_c is moment of inertia of the center body, m_t is tip mass, ρ and EI are the linear mass density and elastic rigidity of the flexible arms. Furthermore, l_0 represents deflection of the flexible arms, represents radius of the center body, and l is distance from the middle of the center body to the tip masses. Flexible arm dynamics also subject to boundary conditions at the root and tip of the arm such as

$$w(x,\ t)=\frac{\partial w(x,\ t)}{\partial t}=0,\ \text{at}\ x=l_0 \quad (2a)$$

$$EI\frac{\partial^2 w}{\partial x^2}=0,\ EI\frac{\partial^3 w}{\partial x^3}=m_t\left(l\ddot{\theta}+\frac{\partial^2 w}{\partial t^2}\right)\ \text{at}\ x=l \quad (2b)$$

2.2 Mathematical modeling

The original hybrid differential equations of motion (Eq. (1)) can be discretized into a finite dimensional mathematical model. The mathematical model is developed for simulation study and the model-based control law design. The flexible displacement is approximated as (Meirovitch, 1990)

$$w(x,\ t)=\sum_{i=1}^{N}\phi_i(x)\,\eta_i(t) \quad (3)$$

where $\phi_i(x)$ $(i=1,\ 2,\ \cdots,\ N)$ are shape functions to be obtained by solving a characteristic equation for a cantilevered beam problem, and $\eta_i(t)$ are generalized coordinates for the flexible deflection.

The finite dimensional equations of motion in matrix form can be written as

$$\begin{bmatrix} I_r & M_{\theta\eta} \\ M_{\eta\theta} & M_{\eta\eta}\end{bmatrix}\begin{Bmatrix}\ddot{\theta}\\ \ddot{\eta}\end{Bmatrix}+\begin{bmatrix}0 & 0\\ 0 & K_{\eta\eta}\end{bmatrix}\begin{Bmatrix}\eta\\ \theta\end{Bmatrix}=\begin{Bmatrix}1\\ 0\end{Bmatrix}u \quad (4)$$

Element mass and stiffness matrices ($M_{\theta\eta}$, $M_{\eta\eta}$, $K_{\eta\eta}$) are computed by using Lagrange's equation, and $\eta=[\eta_1,\ \eta_2,\ \cdots,\ \eta_N]^T$ is the flexible coordinate vector. Equation (4) also can be rewritten in a matrix form as

$$M\ddot{q}+Kq=Fu \quad (5)$$

where M and K are mass and stiffness matrices, respectively, and $F=[1,\ 0,\ 0,\ \cdots,\ 0]^T$ is an input influence vector. State space form of the second order differential equations of motion can be written as

$$\dot{x}=Ax+Bu \quad (6)$$

$$y=Cx+Du \quad (7)$$

where the state vector is defined as $x=[\theta,\ \eta,\ \theta,\ \dot{\eta}]^T$.

An output function of interest is the inertial displacement of the tip mass. During the rotational maneuver, the tip mass displacement is defined in terms of the center body rotation and flexible deflection itself. The total displacement may be an important performance parameter during the attitude maneuver. Mathematically, it can be expressed as

$$\begin{aligned} y&=l\theta+w(l,\ t)\\ &=[l,\ \phi_1(l),\ \phi_2(l),\ \cdots,\ \phi_N(l)]\{\theta,\ \eta_1,\ \eta_2,\ \cdots,\ \eta_N\}^T \quad (8)\\ &=Cx \end{aligned}$$

Similarly, the tip velocity information ($\dot{y}=l\dot{\theta}+\dot{w}(l,\ t)$) can be added to the constraint equation. The additional information may contribute to increasing the observability from a physical viewpoint.

3. Control Law Design

The control law design is primarily targeted to control the tip displacement of the flexible structures in a way that less vibrational motion should be induced by the center torque input. A reference trajectory is generated *a priori*, and corresponding stabilizing control law is designed so that the reference trajectory should be tracked by satisfying the tip displacement constraint equation.

3.1 Reference trajectory

For the reference trajectory generation, we assume a pure rigid body dynamics such as

$$I_r\ddot{\theta}_r=u_r \tag{9}$$

where the reference moment of inertia (I_r) corresponds to that of the pure rigid motion of the whole system as it can be shown from Eq. (1) that

$$I_r=I_c+2\int_{l_0}^{l}\rho x^2dx+2m_tl^2 \tag{10}$$

The reference trajectory output of the system is related to the reference angle as

$$y_r(t)=l\theta_r(t) \tag{11}$$

The reference angle and corresponding control input are originated from a smoothed bang-bang control input with one switching at the half maneuver time. The reference input is defined in the from

$$u_r(t)=N_{\max}f(\Delta t,\ t) \tag{12}$$

where the shaped input torque profile function ($f(t,\Delta t)$) is presented in Fig. 2 (Junkins et al., 1991).

Mathematically, it is expressed as

$$f(\Delta t,t)=\begin{cases}=\left(\frac{t}{\Delta t}\right)^2\left[3-2\left(\frac{t}{\Delta t}\right)\right], & \text{for } 0\le t\le\Delta t\\ =1 & \text{for } \Delta t\le t\le t_f/2-\Delta t=t_1\\ =1-2\left\{\left(\frac{t}{\Delta t}\right)^2\left[3-2\left(\frac{t-t_1}{\Delta t}\right)\right]\right\}, & \text{for } t_1\le t\le t_f/2+\Delta t=t_2\\ =-1 & \text{for } t_2\le t\le t_f-\Delta t=t_3\\ =-1+\left(\frac{t-t_3}{\Delta t}\right)^2\left[3-3\left(\frac{t-t_3}{\Delta t}\right)\right], & \text{for } t_3\le t\le t_f\end{cases}$$

The reference torque profile is obtained from a shaped bang-bang control input. The shaping parameter (α) is used to determine sharpness of the discontinuous control command from $\Delta t=\alpha t_f$. The reference output may include the velocity response also such as

$$y_r(t)=l\dot{\theta}_r \tag{13}$$

Also, combination of both displacement and velocity can be taken as the reference output orconstraint equation. For inverse dynamic problem formulation, the following constraint equation based upon the reference trajectory is established.

$$y(t)=Cx(t)=y_r(t) \tag{14}$$

The constraint equation is used to construct a stabilizing control law.

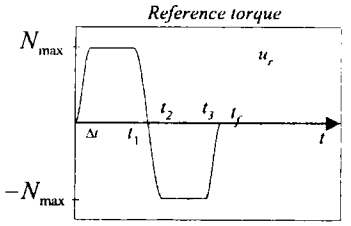

Fig. 2 Shaped input function profile

3.2 Optimal control theory

In order to solve the control problem with the constraint equation (Eq. (14)) and the governing equation in Eq. (6), we elect to employ the optimal control theory. The cost function with the constraint and governing equations satisfied is defined as (Bryson, 1999)

$$J_a=\frac{1}{2}x(t_f)^T\Phi x(t_f)+\frac{1}{2}\int_0^{t_f}[x^TQx+u^TRu+\lambda^T(\dot{x}-Ax-Bu)+\mu^T(Cx-y_r)]dt \tag{15}$$

where λ, μ are Lagrange multipliers for the state and constraint equations, and Φ, Q, R are appropriate weighting matrices, respectively. By variational principle for optimal solution, it is required $\delta J_a=0$, and then we obtain

$$\dot{x}=Ax+Bu \tag{16}$$

$$\dot{\lambda}=-Qx-A^T\lambda-C^T\mu \tag{17}$$

with the following boundary conditions

$$x(0)\in R^n,\ \lambda(t_f)=\Phi x(t_f) \tag{18}$$

The optimal control input is obtained as

$$u(t)=-R^{-1}B^T\lambda \tag{19}$$

The optimal control solution is obtained by solving the following coupled equations simultaneously.

$$\begin{aligned}\dot{x}&=Ax-BR^{-1}B^T\lambda\\ \dot{\lambda}&=-Qx-A^T\lambda-C^T\mu\\ Cx&=y_r\end{aligned}\tag{20}$$

The last equation in Eq. (20) can be used to derive the following relationship

$$C\dot{x}=\dot{y}_r\tag{21}$$

and by using the first equation in Eq. (20) it follows as

$$CAx-CBR^{-1}B^T\lambda=\dot{y}_r\tag{22}$$

Differentiating the above equation one more time yields

$$CA\dot{x}-CBR^{-1}B^T\dot{\lambda}=\ddot{y}_r\tag{23}$$

Substituting the state and co-state equations (Eq. (20)) into Eq. (24), we arrive at

$$\begin{aligned}&(CA^2+CBR^{-1}B^TQ)x+(-CABR^{-1}B^T+CBR^{-1}B^TA^T)\lambda\\&+(CBR^{-1}B^TC^T)\mu=\ddot{y}_r\end{aligned}\tag{24}$$

Therefore, on the condition that the inverse of the matrix $CBR^{-1}B^TC^T$ exists, one can derive the following relationship.

$$\mu(t)=A_1x(t)+A_2\lambda(t)+A_3\ddot{y}_r(t)\tag{25}$$

for which each matrix is given by

$$\begin{aligned}A_1&=-(CBR^{-1}B^TC^T)^{-1}(CA^2+CBR^{-1}B^TQ)\\A_2&=-(CBR^{-1}B^TC^T)^{-1}(-CABR^{-1}B^T+CBR^{-1}B^TA^T)\\A_3&=(CBR^{-1}B^TC^T)^{-1}\end{aligned}$$

Hence, the state and co-state equations can be rewritten as

$$\begin{aligned}\dot{x}&=Ax-BR^{-1}B^T\lambda\\ \dot{\lambda}&=-Qx-A^T\lambda-C^T\mu\\&=-(Q+C^TA_1)x-(A^T+C^TA_2)\lambda-C^TA_3\ddot{y}_r\end{aligned}\tag{26}$$

Hence, Eq. (26) constitutes a two-point boundary value problem for the state and co-state vectors in the optimal control theory with the boundary conditions specified as

$$x(t_0)=x_0,\ \lambda(t_f)=\Phi x(t_f)\tag{27}$$

The boundary conditions are specified at the split time instants (t_0, t_f). For the solution of the boundary value problem, iterative numerical approaches are required. In this work, different solution techniques are proposed to solve the two-point boundary value problem.

3.3 Solution by shooting method

In order to solve the two-pint boundary value problem, a popular method so-called shooting method could be employed. The shooting method provides the initial condition for the co-state at the initial time.

First, the state and co-state equations are combined from Eq. (26) together in the form

$$\begin{aligned}\dot{\xi}&=\begin{Bmatrix}\dot{x}\\ \dot{\lambda}\end{Bmatrix}=\bar{A}\begin{Bmatrix}x\\ \lambda\end{Bmatrix}+\bar{B}u\\&=\bar{A}\xi+\bar{B}u\end{aligned}\tag{28}$$

where $\xi=[x,\ \lambda]^T$, $u\equiv\ddot{y}_r$, and

$$\bar{A}=\begin{bmatrix}H_{11} & H_{12}\\ H_{21} & H_{22}\end{bmatrix},\ \bar{B}=\begin{bmatrix}B_1\\ B_2\end{bmatrix}$$

for which each sub-matrix is defined to be

$$\begin{aligned}&H_{11}=A,\ H_{12}=-BR^{-1}B^T\\&H_{21}=-Q+C^T(CBR^{-1}B^TC^T)^{-1}(CA^2+CBR^{-1}B^TQ)\\&H_{22}=-A^T+C^T(CBR^{-1}B^TCT)^{-1}(-CABR^{-1}BT+CBR^{-1}B^TA^T)\\&B_1=0,\ B_2=-C^T(CBR^{-1}B^TC^T)^{-1}\end{aligned}$$

The step-by-step procedures for the shooting method are given by

i) Guess $\lambda(0)$

ii) Solve

$$\begin{Bmatrix}\dot{x}\\ \dot{\lambda}\end{Bmatrix}=\bar{A}\begin{Bmatrix}x\\ \lambda\end{Bmatrix}+\bar{B}\ddot{y}_r\tag{29}$$

iii) Let

$$\begin{Bmatrix}x\\ \lambda\end{Bmatrix}(t_f)=e^{\bar{A}t}\begin{Bmatrix}x(0)\\ \lambda(0)\end{Bmatrix}+\int_0^{t_f}e^{\bar{A}(t-\tau)}\bar{B}\ddot{y}_r(\tau)\,d\tau\tag{30}$$

or

$$\begin{Bmatrix}x\\ \lambda\end{Bmatrix}(t_f)-\int_0^{t_f}e^{\bar{A}(t_f-\tau)}\bar{B}\ddot{y}_r(\tau)\,d\tau=\begin{bmatrix}\Phi_{11} & \Phi_{12}\\ \Phi_{21} & \Phi_{22}\end{bmatrix}\begin{Bmatrix}x\\ \lambda\end{Bmatrix}(0)\tag{31}$$

iv) Find $\Delta\lambda(0)$ which is a correction for $\lambda(0)$. In other words (Junkins, 1986)

$$\Delta\lambda(0)=-\Phi_{22}^{-1}\lambda(t_f)\tag{32}$$

where

$$\lambda(t_f)=\Phi_{21}x(0)+\Phi_{22}\lambda(0)+f_2(t_f)\tag{33a}$$

$$\begin{Bmatrix}f_1\\ f_2\end{Bmatrix}(t_f)=\int_0^{t_f}e^{\bar{A}(t_f-\tau)}\bar{B}\ddot{y}_r d\tau\tag{33b}$$

Update $\lambda(0)$ in such a way that (Junkins, 1986)

$$\lambda^{i+1}(0)=\lambda^{i}(0)+\Delta\lambda(0) \tag{34}$$

The iteration repeats until convergence is reached. As a special case, one-step iteration for a linear system may suffice to produce the solution. The constraint itself in Eq. (14) is a hard constraint which should be satisfied exactly. In general, the solution process is quite complicated in such a hard constraint case. The numerical solution ends up with unstable modes from the numerical integration for the state and co-state equations. Also, the numerical solution is highly sensitive to the system dynamics. Considering higher flexible modes, the direct approach of numerical solution of the two-point boundary problem may pose serious difficulty in producing the final solution.

3.4 Solution by riccati equation

Another method is to solve the two-point boundary value problem use Riccati equation which starts from the following equations

$$\begin{aligned}\dot{x}&=Ax-BR^{-1}B^{T}\lambda\\ \dot{\lambda}&=-Qx-A^{T}\lambda-C^{T}\mu\\ &=H_{21}x+H_{22}\lambda+B_{2}\ddot{y}_{r}\end{aligned} \tag{35}$$

Assume the Lagrange multiplier λ as (Bryson, 1999)

$$\lambda(t)=P(t)x(t)-\xi(t) \tag{36}$$

where $P(t)$ is a parameter matrix, and $\xi(t)$ is an auxiliary signal for the tracking purpose. Furthermore,

$$\dot{\lambda}=P\dot{x}+\dot{P}x-\dot{\xi} \tag{37}$$

Substituting Eq. (38) into Eq. (36) yields

$$\dot{P}x+P\dot{x}-\dot{\xi}=-H_{21}x+H_{22}(Px-\xi)+B_{2}\ddot{y}_{r} \tag{38}$$

Next using the governing equations for Eq. (40), one can derive the following set of equations

$$\begin{aligned}\dot{P}&=-PA+PBR^{-1}B^{T}P+H_{22}P+H_{21}\\ \dot{\xi}&=PBR^{-1}B^{T}\xi+H_{22}\xi-B_{2}\ddot{y}_{r}\end{aligned} \tag{39}$$

which are subject to

$$P(t_f)=\Phi,\ \xi(t_f)=0 \tag{40}$$

The corresponding control input is then given by

$$u(t)=-R^{-1}B^{T}[Px(t)-\xi(t)] \tag{41}$$

Note that Eqs. (40) can be rewritten as

$$\begin{aligned}\dot{P}&=-PA+[-A^{T}+C^{T}(CGC^{T})^{-1}C(-AG+GA^{T})]P\\ &\quad+PGP+[-Q+C^{T}(CGC^{T})^{-1}C(A^{2}+GQ)]\\ \dot{\xi}&=-[A^{T}-C^{T}(CGC^{T})^{-1}(-AG+GA^{T})-PG]\xi-B_{2}\ddot{y}_{r}(t)\end{aligned} \tag{42}$$

The first part of Eq. (42) looks somewhat similar to the general Riccati equation in a LQR problem. The system matrices are however different. The boundary conditions in Eq. (42) again indicate the problem is another two-point boundary value problem. Numerical approach can be applied to design the parameters $P(t)$, $\xi(t)$ from backward, and they are used finally for forward control input as Eq. (19).

Massive storage requirement for backward integration should be satisfied for actual implementation. Also, the solution is still highly sensitive to the system modeling error. Therefore, the original hard constraint in Eq. (14) needs to be implemented in such a way that stability and robustness of the closed-loop system needs to be ensured. The dynamic observer-based tracking control law in the next section is quite different and more practical approach than the previous cases.

3.4 Observer-based tracking control approach

The direct numerical approach to solve the two-point boundary value problem is rather impractical from several perspectives. Therefore, a more reliable and stable method should be developed. As a principal avenue, we propose so-called observer-based tracking control law approach.

The state equation again is given by Eq. (6) while the constraint equation (Eq. (14)) is instead defined as the output equation in a way that

$$y(t)=Cx=y_{d}(t) \tag{43}$$

where the desired output (y_d) is the pre-defined tip displacement and/or tip velocities as explained already. The output is used as an input to a dynamic observer written as

$$\dot{\hat{x}}=A\hat{x}+L(y-C\hat{x})=A\hat{x}+LC(x-\hat{x}) \\ =A\hat{x}+L(y_d-C\hat{x}) \quad (44)$$

where L is a typical observer gain and $\hat{x}$ is the observer state. First we design the observer gain L such that the closed-loop system $A-LC$ is stabilized. The closed-loop system dynamics are prescribed as

$$\dot{\hat{x}}=(A-LC)\hat{x}+Ly_d \quad (45)$$

The observer state satisfies the closed-loop system dynamics in the sense of LQR stability with inherent robustness. Moreover, by subtracting the observer equation (Eq. (44)) from the state equation (Eq. (16)) we obtain

$$\dot{e}=(A-LC)e+Bu \quad (46)$$

where $e=x-\hat{x}$ represents the error state between the state and observer. Now the goal of controller design is to find the control command in such a way that $e(\infty)\rightarrow 0$. The plant state converges to the observer state asymptotically. This will eventually bring the state vector satisfies the constraint equation $(y=y_d)$. That is to say, the state approaches the observer, and the observer equation satisfies the output equation. Thus we attempt to design a feedback control law in the form

$$u=-Ke \quad (47)$$

so that the closed-loop system $A-LC-BK$ for the error state is stabilized in the sense of a typical LQR state feedback design. It should be noted that the closed-loop observer dynamics $A-LC$ is already a stable system. But the control input still should be constructed, and a particular choice is to make the error state (e) goes to zero by the control input so that the output response of the actual system follows that of the observer. The compound system consists of state and observer dynamics, and therefore can be rewritten as

$$\begin{Bmatrix}\dot{x}\\ \dot{\hat{x}}\end{Bmatrix}=\begin{bmatrix}A-BK & BK\\ 0 & A-LC\end{bmatrix}\begin{Bmatrix}x\\ \hat{x}\end{Bmatrix}+\begin{bmatrix}0\\ L\end{bmatrix}y_d \quad (48)$$

The final state equation is therefore in the form a stabilized system subject to external input (y_d). The feedback gains (L, K) can be designed by the regular LQR design approach. Hence, the observer-based approach is more attractive than the direct method for which we tried to solve the two-point boundary value problem numerically. The original constraint in the observer-based tracking control method has been relaxed by the asymptotic stability of the feedback system. The error state tends to converge to zero asymptotically governed by the closed-loop dynamics, so that the constraints equation is also satisfied with stabilized responses. The principal idea of this study is to make use of observer dynamics for reference trajectory generation. And then robust feedback control law is applied to track the observer system. Even if the control theory itself is well known, but the main idea using an observer as a reference trajectory should be paid attention in this study.

4. Simulation and Analysis

Simulation is conducted to verify the proposed control approach. We present the observer-based tracking control results only due to the difficulty in directly solving the two-point boundary value problem. First the model spacecraft data are given by $\rho=8.55$ kg/m, $EI=1{,}620$ N/m^2, $I_c=80$ kgm^2, $m_t=1.0$ kg, $l_0=1$ m, $l=6$ m, and $m_t=1$ kg, respectively. The finite dimensional mathematical model is derived by using the assumed mode method as explained in Eq. (5). The three shape functions $(\phi_i(x),\ i=1, 2, 3)$ are obtained by solving an eigenvalue problem for a canti-levered beam with a tip mass. The simple Euler-beam bending dynamics in conjunction with the boundary conditions are used to establish the eigenvalue problem to obtain the shape functions. Consequently, the linearized second order system dynamics and state space form are generated. The mass and stiffness matrices are computed as

$$M=\begin{bmatrix}1377.5 & 322.83 & 78.325 & 36.590\\ 322.83 & 87.378 & 6.91\times10^{-13} & 9.48\times10^{-12}\\ 78.325 & 6.91\times10^{-13} & 87.109 & 4.18\times10^{-11}\\ 36.590 & 9.48\times10^{-12} & 4.18\times10^{-11} & 86.904\end{bmatrix}$$

$$K=\begin{bmatrix}0 & 0 & 0 & 0\\ 0 & 299.38 & 0 & 2.35\times10^{-10}\\ 0 & 0 & 11{,}798 & 2.37\times^{10-8}\\ 0 & 2.35\times10^{-10} & 2.37\times10^{-8} & 92{,}768\end{bmatrix}$$

The undamped natural frequencies for the given matrices are computed as 0, 4.88, 15.17, and 35.44 rad/sec, respectively. The maximum torque limit (N_{max}) and torque shaping parameter (a) are selected to be 15 N-m and 0.05, respectively. The reference constraint equation is represented in the form

$$y=Cx=y_d=\begin{bmatrix} y_r \\ \dot{y}_r \end{bmatrix} \tag{49}$$

Also the corresponding output matrix is given by

$$C=\begin{bmatrix} l, \phi_1(l), \phi_2(l), \phi_3(l), 0, 0, 0, 0 \\ 0, 0, 0, 0, l, \phi_1(l), \phi_2(l), \phi_3(l) \end{bmatrix} \tag{50}$$

First, the dynamic observer is designed by using the system and output matrices (A, C). Then the state feedback design is followed by the closed-loop observer dynamics. The state and observer equations are combined into a final system for simulation work. The simulation time is set to 50 seconds enough for 60 degrees rotational maneuver.

First, pure open-loop maneuver with applied torque in Eq. (9) is examined. The time response is presented in Fig. 3.

In order to reflect a practical situation, a small level of disturbing torque is added to the original control torque. The center body angle response in Fig. 3 illustrates the inherent disadvantage of the open-loop control. Unmodelled disturbance usually tends to degrade pointing performance significantly.

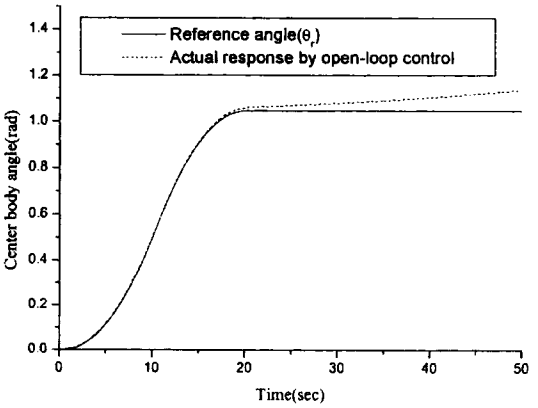

Fig. 3 Simulation results with the pure open-loop torque with small disturbance

Next the observer-based tracking control law design results are presented in Fig. 4. The center body angle shows satisfactory tracking performance over the given reference trajectory. The disturbance input identical to that of the pure open-loop simulation is added to the control command in this case. Satisfactory tracking performance under the existence of external disturbance is achieved in the simulation results of Fig. 4.

Time responses of the original constraint and actual responses are plotted in Fig. 5. Both displacement and velocity constraints are plotted. The constraint dynamics are determined by the observer and feedback control gains.

Control input histories are displayed in Fig. 6. The pure open-loop and feedback tracking control command are displayed together. Delayed

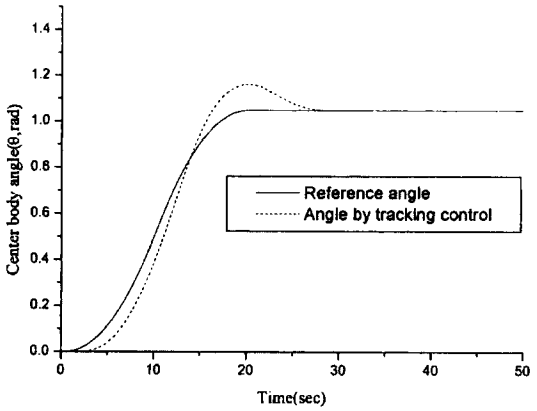

Fig. 4 Center body angle response by the tracking control law

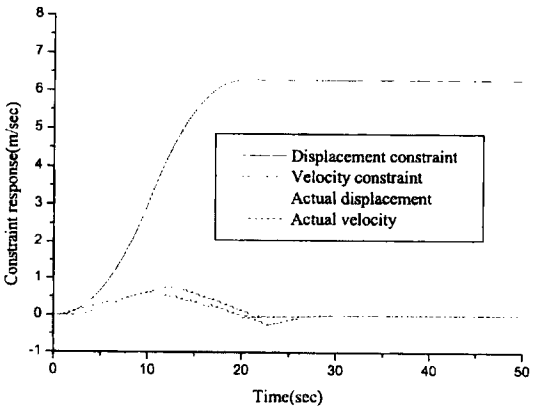

Fig. 5 Responses of the constraint equation

response in the feedback control could be improved by designing a better gain set for the observer and state feedback.

Responses of two flexible modes (η_1, η_3) are presented in Fig. 7. The flexible modes are also stabilized by the state feedback and observer in conjunction with the constraint equation.

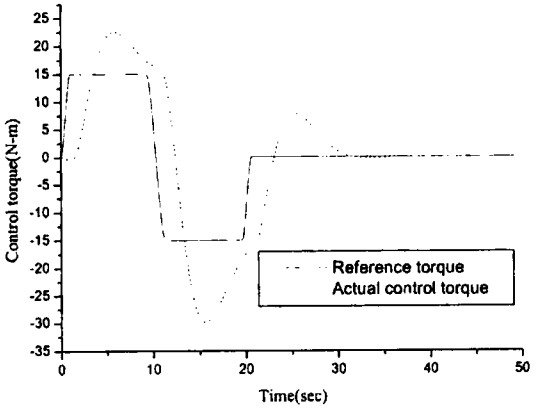

Fig. 6 Control command histories

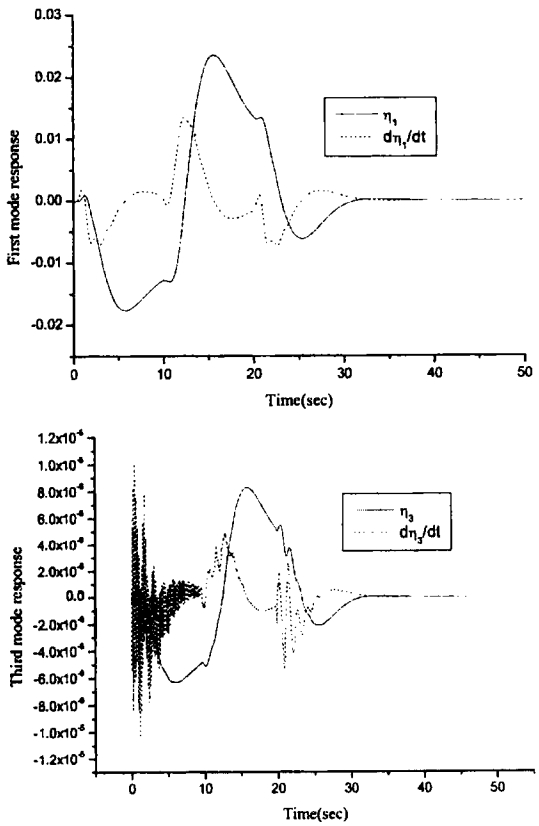

Fig. 7 Responses of the flexible states

It is believed that the overall performance of the combined system may be similar to a general LQR-based control law. This is because both observer for the reference trajectory generation and feedback control for stabilization of the whole system are designed by LQR synthesis technique.

5. Conclusions

The constraint equation for the tip displacement of a flexible spacecraft model was used to derive a stable tracking control law. A dynamic observer with the measurement input replaced by the constrained output history plays the role of a model system. The feedback control law which takes the error between the observer state and actual system state results in a stable closed-loop system. Simulation results are presented to validate the proposed idea. Hence, the observer-based tracking control law with stabilized closed-loop system response leads to a more attractive solution than directly solving the two-point boundary value problem in our problem.

Acknowledgment

The present work was supported by National Research Lab.(NRL) Program (M1-0203-00-0006) by the Ministry of Science and Technology, Korea. Authors fully appreciate the financial support.

References

Agrawal, B. N. and Bang, H., 1995, "Robust Closed-loop Control Design for Spacecraft Maneuver Using On-Off Thrusters," *Journal of Guidance, Control, and Dynamics*, Vol. 18, No. 6, pp. 1336~1349.

Breakwell, J. A., 1981, "Optimal Feedback Control for Flexible Spacecraft," *Journal of Guidance, Control, and Dynamics*, Vol. 4, No. 5, pp. 427~479.

Bryson, A. E., 1999, *Dynamic Optimization*, Addison-Wesley.

Byers, R. M., Vadali, S. R. and Junkins, J. L., 1989, "Near-Minimum-Time Closed-Loop Slewing of Flexible Spacecraft," *Journal of Guidance, Control, and Dynamics*, Vol. 12, No. 6, pp. 858~865.

Fujii, H., Ohtsuka, T. and Udo, S., 1989, "Mission Function Control for Slew Maneuver Experiment," *Journal of Guidance, Control, and Dynamics*, Vol. 12, No. 6, pp. 858~865.

Junkins, J. L., Rahman, Z., Bang, H. and Hecht, N., 1991, "Near-Minimum-Time Control of Distributed Parameter Systems : Analytical and Experimental Results," *Journal of Guidance, Control, and Dynamics*, Vol. 14, No. 2, pp. 406~415.

Junkins, J. L. and Turner, J. D., 1986, *Optimal Spacecraft Rotational Maneuvers*, Elsevier Science Publisher B. V.

Kim, Y., Suk, J. Kim, S. and Junkins, J. L., 1997, "Near-Minimum-Time Control of Smart Structures for Slew Maneuver," *Journal of the Astronautical Sciences*, Vol. 45, No. 1, pp. 91~111.

Meirovitch, L. and Quinn, R., 1987, "Maneuvering and Vibration Control of Flexible Spacecraft," *Journal of Astronautical Sciences*, Vol. 35, No. 3, pp. 301~328.

Meirovitch, L., 1990, *Dynamics and Control of Structures*, Wiley Interscience, New York.

Singh, G., Kabamba, P. and McClamroch, N., 1989, "Planar Time Optimal Slewing Maneuvers of Flexible Spacecraft," *Journal of Guidance, Control, and Dynamics*, Vol. 12, No. 1, pp. 71~81.

Sung, Y. G., Lee, J. W. and Kim, H. M., 2001, "A Robust Control Approach for Maneuvering a Flexible Spacecraft," *KSME International Journal*, Vol. 15, No. 2, pp. 143~151.

Vadali, S. R., 1984, "Feedback Control of Flexible Spacecraft Large Angle Maneuvers Using the Liapunov Theory," *Proceedings of the 1984 American Control Conference, Inst. of Electrical and Electronics Engineers*, Piscataway, NJ, pp. 1674~1678.

VanderVelde, W. and He, J., 1983, "Design of Space Structure Control Systems Using On-Off Thrusters," *Journal of Guidance, Control, and Dynamics*, Vol. 6, No. 1, pp. 759~775.

Wie, B., Sinha, R. and Liu, Q., 1993, "Robust Time-Optimal Control of Uncertain Structural Dynamic Systems," *Journal of Guidance, Control, and Dynamics*, Vol. 15, No. 5, pp. 980~983.